Inorganic Chemistry

Article

Pt(II) Diimine Chromophores with Perfluorinated Thiolate Ligands: Nature and Dynamics of the Charge-Transfer-to-Diimine Lowest Excited State

Julia A. Weinstein,[*,†,‡] Alexander J. Blake,[†] E. Stephen Davies,[†] Adrienne L. Davis,[†] Michael W. George,[*,†] David C. Grills,[†] Igor V. Lileev,[‡] Alexander M. Maksimov,[§] Pavel Matousek,[||] Mikhail Ya. Mel'nikov,[‡] Anthony W. Parker,[||] Vyacheslav E. Platonov,[§] Michael Towrie,[||] Claire Wilson,[†] and Natalia N. Zheligovskaya[‡]

School of Chemistry, University of Nottingham, Nottingham NG7 2RD, United Kingdom, Department of Chemistry, Moscow Lomonosov State University, Moscow 119899, Russia, Novosibirsk Institute of Organic Chemistry, 630090, Novosibirsk, Russia, and CCLRC, Rutherford Appleton Laboratory, Chilton, Didcot, Oxfordshire OX11 0QX, United Kingdom

The synthesis of new Pt(II) diimine complexes bearing perfluorinated thiolate ligands, $Pt^{II}(NN)(4\text{-}X\text{-}C_6F_4\text{-}S)_2$, where NN = 2,2′-bipyridine or 1,10-phenanthroline and X = F or CN, is reported, together with an investigation of the nature and dynamics of their lowest excited states. A combined UV−vis, (spectro)electrochemical, resonance Raman, and time-resolved infrared (TRIR) study has suggested that the HOMO is mainly composed of thiolate(π)/S(p)/Pt(d) orbitals and that the LUMO is largely localized on the π^* (diimine) orbital, thus revealing the {charge-transfer-to-diimine} nature of the lowest excited state. An enhancement of the thiolate ring vibrations, C−F vibrations, and the vibration of the CN-substituent on the thiolate moiety was observed in the resonance Raman spectra, whereas no such enhancement was seen for the nonfluorinated analogues. Thus, the introduction of fluorine substituents on the thiolate moiety probably leads to a more pronounced contribution of the intrathiolate modes to the HOMO compared to the analogous complexes with nonfluorinated thiolates. Furthermore, the introduction of the *p*-CN group into the thiolate moiety has allowed the dynamics of the lowest excited state of $Pt(bpy)(4\text{-}CN\text{-}C_6F_4\text{-}S)_2$ to be monitored by picosecond TRIR spectroscopy. The dynamics of the lowest {charge-transfer-to-diimine} excited state are governed by ca. 2-ps vibrational cooling and 35-ps back electron transfer.

Introduction

Charge-separated excited states are key intermediates in a wide variety of processes including bimolecular photo-catalysis and light−chemical energy conversion.[1] An understanding of the primary photophysical processes in such systems is a prerequisite for the rational design of charge-separated excited states with specific properties. Research into metal-chromophore-based systems has focused mainly on d[6] Ru(II), Os(II), and Re(I) diimines, as has been reviewed in

detail elsewhere.[1−3] Coordinatively unsaturated Pt(II) d[8] diimine chromophores have received much less attention,[4−9] partly due to the low solubility many of these complexes exhibit. However, Pt(II) chromophores have shown significant potential

---

* Authors to whom correspondence should be addressed. E-mail: julia.weinstein@nottingham.ac.uk (J.A.W.); mike.george@nottingham.ac.uk (M.W.G.).
† University of Nottingham.
‡ Moscow Lomonosov State University.
§ Novosibirsk Institute of Organic Chemistry.
|| Rutherford Appleton Laboratory.

(1) (a) *Electron Transfer in Chemistry*; Balzani, V., Ed.; Wiley-VCH: Weinheim, Chichester, 2001. (b) *Organic and Inorganic Photochemistry*; Ramamurthy, V., Schanze, K. S., Eds.; Marcel Dekker: New York, 1998.

(2) Ballardini, R.; Balzani, V.; Credi, A.; Gandolfi, M. T.; Venturi, M. *Acc. Chem. Res.* **2001**, *34*, 445.

(3) Chen, P. Y.; Meyer, T. J. *Chem. Rev.* **1998**, *98*, 1439.

(4) (a) Vogler, C.; Schwederski, B.; Klein, A.; Kaim, W. *J. Organomet. Chem.* **1992**, *436*, 367. (b) Braterman, P. S.; Song, J. I.; Vogler, C.; Kaim, W. *Inorg. Chem.* **1992**, *31*, 222. (c) Connick, W. B.; Gray, H. B. *J. Am. Chem. Soc.* **1997**, *119*, 11620. (d) Kunkely, H.; Vogler, A. *Inorg. Chim. Acta* **1997**, *264*, 305. (e) Base, K.; Tierney, M. T.; Fort, A.; Muller, J.; Grinstaff, M. W. *Inorg. Chem.* **1999**, *38*, 287. (f) Klein, A.; Scheiring, T.; Kaim, W. *Z. Anorg. Allg. Chem.* **1999**, *625*, 1177.

(5) (a) Vogler, A.; Kunkely, H.; Hlavatsch, J.; Merz, A. *Inorg. Chem.* **1984**, *23*, 506. (b) Tzeng, B.-C.; Fu, W.-F.; Che, C.-M.; Chao, H.-Y.; Cheung, K.-K.; Peng, S.-M. *J. Chem. Soc., Dalton Trans.* **1999**, 1017.

(6) Zhang, Y.; Ley, K. D.; Schanze, K. S. *Inorg. Chem.* **1996**, *35*, 7102.

(7) Base, K.; Grinstaff, M. W. *Inorg. Chem.* **1998**, *37*, 1432.

(8) Hissler, M.; McGarrah, J. E.; Connick, W. B.; Geiger, D. K.; Cummings, S. D.; Eisenberg, R. *Coord. Chem. Rev.* **2000**, *208*, 115.

(9) Whittle, C. E.; Weinstein, J. A.; George, M. W.; Schanze, K. S. *Inorg. Chem.* **2001**, *40*, 4053.

as DNA intercalators,[10] as building blocks in polynuclear transition metal systems designed for electron/energy transfer,[8,11] and as sensing devices.[12]

The nature and dynamics of the lowest excited state is an issue of particular importance for metal chromophores since these possess a manifold of low-lying excited states of different origin.[13] The nature of the lowest excited state in Pt[II] diimine dithiolates, where diimine is a derivative of 2,2′-bipyridine (bpy) or 1,10-phenanthroline (phen), has previously been assigned as either {charge-transfer-to-diimine}[8] or ligand—ligand charge transfer (LLCT).[5] The lowest excited state for flexible bis-thiolate systems, Pt(bpy)(4-X—$C_6H_4S)_2$, has also been shown to be {charge-transfer-to-diimine} with the highest occupied molecular orbital (HOMO) being mainly of S(lone pair)/Pt(d) origin.[7,14,15] The desired properties of excited states such as their lifetime or degree of charge separation can be achieved by the careful design and modification of the ligands.

Pt[II] diimine complexes that show emission in fluid solution on the nanosecond or longer time scale include some dithiolates,[8,16−18] acetylides,[8,9,19] and cyanides.[20] However, the majority of Pt[II] excited states are short lived and the elucidation of their dynamics requires fast spectroscopic methods.

Time-resolved infrared (TRIR) spectroscopy has proved to be a powerful technique for probing the electronic redistribution which occurs upon formation of excited states of coordination compounds, particularly those bearing IR reporter ligands such as CO or CN.[21−23] Peripheral IR

reporter groups such as carboxylic acids and esters on substituted diimine ligands have also been used[24−26] to indirectly probe charge transfer-processes using both nanosecond- and picosecond-TRIR. However, there have been relatively few TRIR investigations of Pt[II] diimine chromophores.[9,26,27]

Herein, we present an investigation into the photophysics of Pt[II] diimines bearing perfluorinated[28] thiolate ligands. We have used UV−vis absorption spectroscopy, resonance Raman spectroscopy, and (spectro)electrochemistry to probe the origin of the lowest excited state in these new, highly soluble fluorinated compounds. Our results are consistent with previously reported data on the related non-fluorinated Pt(diimine)(bis)thiolates.

We have introduced conjugated perfluorinated thiolate ligands to decrease the donor capacity of the thiolate ligand moiety and to produce a more charge-delocalized excited state. Furthermore, the introduction of the *para*-CN group into the thiolate moiety has allowed the dynamics of the lowest excited state of Pt(bpy)(4-CN—$C_6F_4S)_2$ to be monitored in solution at room temperature by picosecond TRIR spectroscopy.

Experimental Section

Materials. All solvents were distilled over CaH_2 under a dry nitrogen atmosphere prior to use. 2,2′-Bipyridine, 1,10-phenanthroline, ferrocene (Aldrich), potassium *tert*-butoxide, and hexamethylenetetraamine (hmt) (Sigma) were used as received. For electrochemical experiments, anhydrous dimethylformamide (DMF) (Fluka) was used as received. The supporting electrolyte, [NBu₄]-[BF₄], was prepared from [NBu₄]Cl and Na[BF₄] (Aldrich) and recrystallized twice from dichloromethane.[29]

A modified literature procedure was employed to synthesize Pt-(diimine)Cl₂ from K₂[PtCl₄] and the corresponding diimine.[30] The thiolate ligands C_6F_5SH and 4-CN—C_6F_4SH were synthesized as described elsewhere.[31]

Synthesis of Pt(NN)(4-X—$C_6F_4S)_2$, NN = 2,2′-Bipyridine or 1,10-Phenanthroline, X = F or CN. Pt(bpy)($C_6F_5S)_2$, 1. To a mixture of Pt(bpy)Cl₂ (422 mg, 1 mmol) and hexamethylenetet-

(10) (a) Jennette, K. W.; Gill, J. T.; Sadownick, J. A.; Lippard, S. J. *J. Am. Chem. Soc.* **1976**, *98*, 6159. (b) Peyratout, C. S.; Aldridge, T. K.; Crites, D. K.; McMillin, D. R. *Inorg. Chem.* **1995**, *34*, 4484. (c) Che, C.-M.; Yang, M. S.; Wong, K. H.; Chan, H. L.; Lam, W. *Chem.-Eur. J.* **1999**, *5*, 3350. (d) Cusumano, M.; Di Pietro, M. L.; Giannetto, A.; Romano, F. *Inorg. Chem.* **2000**, *39*, 50.

(11) (a) Yam, V. W. W.; Lee, V. W. M.; Cheung, K. K. *J. Chem. Soc., Chem. Commun.* **1995**, 801. (b) Harriman, A.; Ziessel, R. *Chem. Commun.* **1996**, 1707. (c) Harriman, A.; Ziessel, R. *Coord. Chem. Rev.* **1998**, *171*, 331.

(12) (a) Wong, K. H.; Chan, M. C. W.; Che, C.-M. *Chem.−Eur. J.* **1999**, *5*, 2845. (b) Bedlek-Anslow, J. M.; Hubner, J. P.; Carroll, B. F.; Schanze, K. S. *Langmuir* **2000**, *16*, 9137. (c) Van Houten, K. A.; Walters, K. A.; Schanze, K. S.; Pilato, R. S. *J. Fluoresc.* **2000**, *10*, 35. (d) Yam, V. W. W.; Tang, R. P. L.; Wong, K. M. C.; Cheung, K. K. *Organometallics* **2001**, *20*, 4476.

(13) Vlček, A. *Coord. Chem. Rev.* **2000**, *200*, 933.

(14) Weinstein, J. A.; Zheligovskaya, N. N.; Mel'nikov, M. Y.; Hartl, F. *J. Chem. Soc., Dalton Trans.* **1998**, 2459.

(15) Weinstein, J. A.; Zheligovskaya, N. N.; Lileev, I. V.; Galin, A. M.; Mel'nikov, M. Y. *Russ. J. Inorg. Chem., Engl. Transl.* **1998**, *43*, 1361.

(16) (a) Huertas, S.; Hissler, M.; McGarrah, J. E.; Lachicotte, R. J.; Eisenberg, R. *Inorg. Chem.* **2001**, *40*, 1183. (b) Paw, W.; Lachicotte, R. J.; Eisenberg, R. *Inorg. Chem.* **1998**, *37*, 4139. (c) Bevilacqua, J. M.; Eisenberg, R. *Inorg. Chem.* **1994**, *33*, 2913.

(17) Zuleta, J. A.; Bevilacqua, J. M.; Proserpio, D. M.; Harvey, P. D.; Eisenberg, R. *Inorg. Chem.* **1992**, *31*, 2396.

(18) Cummings, S. D.; Eisenberg, R. *J. Am. Chem. Soc.* **1996**, *118*, 1949.

(19) (a) Chan, C. W.; Cheng, L. K.; Che, C. M. *Coord. Chem. Rev.* **1994**, *132*, 87. (b) Hissler, M.; Connick, W. B.; Geiger, D. K.; McGarrah, J. E.; Lipa, D.; Lachicotte, R. J.; Eisenberg, R. *Inorg. Chem.* **2000**, *39*, 447. (c) Chan, S. C.; Chan, M. C. W.; Wang, Y.; Che, C. M.; Cheung, K. K.; Zhu, N. Y. *Chem.−Eur. J.* **2001**, *7*, 4180. (d) Fleeman, W. L.; Connick, W. B. *Comments Inorg. Chem.* **2002**, *23*, 205. (e) Pomestchenko, I. E.; Luman, C. R.; Hissler, M.; Ziessel, R.; Castellano, F. N. *Inorg. Chem.* **2003**, *42*, 1394. (f) Wadas, T. J.; Lachicotte, R. J.; Eisenbeg, R. *Inorg. Chem.* **2003**, *42*, 3772.

(20) Pettijohn, C. N.; Jochnowitz, E. B.; Chuong, B.; Nagle, J. K.; Vogler, A. *Coord. Chem. Rev.* **1998**, *171*, 85.

(21) George, M. W.; Turner, J. J. *Coord. Chem. Rev.* **1998**, *177*, 201.

(22) Schoonover, J. R.; Gordon, K. C.; Argazzi, R.; Woodruff, W. H.; Peterson, K. A.; Bignozzi, C. A.; Dyer, R. B.; Meyer, T. J. *J. Am. Chem. Soc.* **1993**, *115*, 10996.

(23) Kuimova, M. K.; Mel'nikov, M. Y.; Weinstein, J. A.; George, M. W. *J. Chem. Soc., Dalton Trans.* **2002**, 2857.

(24) (a) Heimer, T. A.; Heilweil, E. J. *J. Phys. Chem. B* **1997**, *101*, 10990. (b) Khan, S. I.; Beilstein, A. E.; Smith, G. D.; Sykora, M.; Grinstaff, M. W. *Inorg. Chem.* **1999**, *38*, 2411. (c) Smith, G. D.; Maxwell, K. A.; DeSimone, J. M.; Meyer, T. J.; Palmer, R. A. *Inorg. Chem.* **2000**, *39*, 893.

(25) (a) Chen, P. Y.; Omberg, K. M.; Kavaliunas, D. A.; Treadway, J. A.; Palmer, R. A.; Meyer, T. J. *Inorg. Chem.* **1997**, *36*, 954. (b) Omberg, K. M.; Smith, G. D.; Kavaliunas, D. A.; Chen, P. Y.; Treadway, J. A.; Schoonover, J. R.; Palmer, R. A.; Meyer, T. J. *Inorg. Chem.* **1999**, *38*, 951.

(26) Weinstein, J. A.; Grills, D. C.; Towrie, M.; Matousek, P.; Parker, A. W.; George, M. W. *Chem. Commun.* **2002**, 382.

(27) Smith, G. D.; Hutson, M. S.; Lu, Y.; Tierney, M. T.; Grinstaff, M. W.; Palmer, R. A. *Appl. Spectrosc.* **2001**, *55*, 637.

(28) (a) Torrens, H. *Coord. Chem. Rev.* **2000**, *196*, 331. (b) Martin, E.; Toledo, B.; Torrens, H.; Lahoz, F.; Terreros, P. *Polyhedron* **1998**, *17*, 4091.

(29) Kubas, J. *Inorg. Synth.* **1990**, *28*, 68.

(30) Morgan, G. T.; Burstal, F. H. *J. Chem. Soc.* **1934**, 965.

(31) Maksimov, A. M.; Platonov, V. E. www.flourine.ru\Notes\archive.html, 1999.
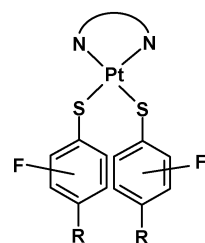
	NN	R
1	2,2'-bipyridine	F
2	2,2'-bipyridine	CN
3	1,10-phenanthroline	F
4	1,10-phenanthroline	CN

raamine (280 mg, 2 mmol) in degassed EtOH (100 cm³), a degassed solution of C_6F_5SH (2.4 mmol) containing KO^tBu (269 mg, 2.4 mmol) in 20 cm³ of EtOH was added dropwise. The reaction mixture was heated on a water bath under a nitrogen atmosphere with continuous stirring for ca. 4 h. The resulting orange precipitate was filtered, washed with hot water (3 × 20 cm³) and ethanol (2 × 20 cm³), and dried under vacuum overnight. Yield 78%. ^1H NMR [$(CD_3)_2SO$]: $\delta = 9.62$ (dd, 2H), 8.75 (dd, 2H), 8.47 (t, 2H), 7.92 (t, 2H). ^{19}F NMR: $\delta = -130.52$ (2F), -160.15 (1F), -163.04 (2F). ^{195}Pt NMR: $\delta = -3245$. Anal. Calcd for $C_{22}H_8F_{10}N_2PtS_2$: C, 35.25; H, 1.07; N, 3.74. Found: C, 35.02; H, 0.96; N, 3.40.

Pt(bpy)(4-CN−C_6F_4S)$_2$, 2. The dark-yellow complex was prepared using the same procedure as for Pt(bpy)(C_6F_5S)$_2$. Yield 82%. ^1H NMR [$(CD_3)_2SO$]: $\delta = 9.49$ (dd, 2H), 8.74 (d, 2H), 8.48 (t, 2H), 7.89 (t, 2H). ^{19}F NMR: $\delta = -131.71$ (2F), -138.25 (2F). ^{195}Pt NMR: $\delta = -3178$. Anal. Calcd for $C_{24}H_8F_8N_4PtS_2$: C, 37.77; H, 1.05; N, 7.34. Found: C, 37.58; H, 0.89; N, 6.78.

Pt(phen)(C_6F_5S)$_2$, 3. The orange complex was prepared using the same procedure as for Pt(bpy)(C_6F_5S)$_2$. Yield 80%. ^1H NMR [$(CD_3)_2SO$]: $\delta = 9.70$ (dd, 2H), 9.10 (dd, 2H), 8.25 (t, 2H), 8.35 (s, 2H). ^{19}F NMR: $\delta = -130.31$ (2F), -160.03 (1F), -163.01 (2F). ^{195}Pt NMR: $\delta = -3275$. Anal. Calcd for $C_{24}H_8F_{10}N_2PtS_2$: C, 37.26; H, 1,03; N, 3.62. Found: C, 37.06; H, 0.98; N, 3.76.

Pt(phen)(4-CN−C_6F_4S)$_2$, 4. To a mixture of solid Pt(phen)Cl$_2$ (170 mg, 0.38 mmol) and hmt (106 mg, 0.76 mmol) in degassed THF (100 cm³), a degassed solution of 4-CN−C_6F_4SH (174 mg, 0.84 mmol) and KO^tBu (94 mg, 0.84 mmol) was added dropwise. The reaction mixture was stirred at reflux for ca. 7 h, with a gradual change of color from yellow to orange. The volume of THF was then reduced, and the resulting orange precipitate was filtered off, washed with hot water (3 × 30 cm³) and ethanol (2 × 20 cm³), and dried under vacuum overnight. The product was then purified by column chromatography on silica gel with CH_2Cl_2/CH_3CN (10:1) as an eluent to yield a bright-orange solid. Yield 70%. ^1H NMR [$(CD_3)_2SO$]: $\delta = 9.75$ (dd, 2H), 9.12 (dd, 2H), 8.37 (s), 8.25 (dd, 2H). ^{19}F NMR: $\delta = -131.4$ (2F), -138.2 (2F). ^{195}Pt NMR: $\delta = -3215$. The mass calculated for $C_{24}H_8F_{10}N_2PtS_2$ based on ^{195}Pt, ^{12}C, ^1H, ^{14}N, ^{19}F, ^{32}S = 787. ES MS: found $m/z^+ = 787$ as the most intense peak.

Compounds **1**−**4** are stable as solids and in deaerated solutions of organic solvents. The $^{195}Pt-\{^1H\}$ NMR spectra exhibit the singlet resonance in the region expected for Pt^{II} imine thiolate compounds.[32] Molar conductivity measurements revealed the compounds studied to be nonelectrolytes, stable as 1 mM ethanolic solutions for at least 24 h.

Methods and Instrumentation. ^1H, ^{19}F, and $^{195}Pt-\{^1H\}$ NMR spectra were recorded on a Bruker 300 MHz spectrometer at 298 K in DMSO-d_6 unless otherwise stated. ^{19}F chemical shifts are reported vs CFCl$_3$ ($\delta = 0$). ^{195}Pt NMR shifts were measured at ambient temperature (**1** and **2**) or 298 K (**3** and **4**) and were

referenced according to the 2001 IUPAC recommendations[33] with $\Xi = 21.496784$.

Raman data were collected on a Nicolet-Almega instrument using 785 nm excitation; the band positions are determined by means of internal calibration. Resonance Raman data were collected from spinning KNO$_3$ pellets (approximately 200 mg of KNO$_3$ and 15 mg of platinum complex) at room temperature upon excitation with the 457.9 and 488.1 nm lines of a Spectra Physics model 2016 Ar$^+$ laser. The incident laser power was varied from 90 to 100 mW. The data were collected using a Dilor Modular spectrometer with backscattering geometry and a charge-coupled device (CCD) detection system. The positions of the bands are reported relative to the KNO$_3$ bands at 1051.3 and 716.4 cm^{-1}.

Crystals of **2** suitable for X-ray diffraction analysis were obtained by slow diffusion of pentane into a 2-Me-THF solution at room temperature. A yellow, prismatic crystal, 0.30 × 0.09 × 0.04 mm, was mounted in perfluoropolyether oil. Data were collected at 150 K on a Bruker SMART1000 CCD area detector diffractometer equipped with an Oxford Cryosystems open-flow nitrogen cryostat.[34] Data were corrected for Lorentz and polarization effects and for absorption, using a semiempirical method[35] (T range 0.483−0.774). The structure was solved by direct methods,[36] and the structure was refined using full-matrix least squares refinement against F^2. All non-H atoms were refined with anisotropic displacement parameters and H atoms placed in geometrically calculated positions and refined as part of a riding model, with $U(H)_{iso} = 1.2U_{eq}(C)$.[37] $C_{24}H_8F_8N_4PtS_2$, $M = 763.55$, triclinic, $a = 8.768(2)$ Å, $b = 11.084(3)$ Å, $c = 13.007(3)$ Å, $\alpha = 111.553(3)°$, $\beta = 95.589(3)°$, $\gamma = 98.220(3)°$, $U = 1148.1(5)$ Å^3, $T = 150$ K, space group $P\bar{1}$ (no. 2), $Z = 2$, μ (Mo Kα) = 6.382 mm^{-1}, 7283 reflections measured, 5135 unique ($R_{int} = 0.029$), which were used in all calculations. The final wR$_2(F^2)$ was 0.0474 for all data, R$_1$ (F) was 0.0333 for 4074 observed data where $I > 2\sigma(I)$. CCDC reference number: 217858.

The electrochemical and (spectro)electrochemical samples were prepared in DMF under an inert atmosphere using Schlenk techniques.

Standard cyclic voltammetry was carried out under an atmosphere of argon using a three-electrode arrangement in a single compartment cell. A glassy carbon working electrode, a Pt wire secondary electrode, and a saturated calomel electrode (S.C.E.) were chemically isolated from the test solution via a bridge tube containing electrolyte solution with a porous Vycor frit. The solutions were 10^{-3} M in the test compound and 0.2 M in [NBu$_4$][BF$_4$] as supporting electrolyte. The redox potentials are quoted versus the ferrocenium−ferrocene couple;[38] $E_{1/2}$ ([Cp$_2$Fe]$^+$/[Cp$_2$Fe]) was 0.493 V vs S.C.E. under these conditions.

The UV−vis spectroelectrochemical experiments were carried out with an optically transparent thin-layer electrochemical (OT-TLE) cell[39] (modified quartz cuvette, with 0.5 mm optical path length). The cell comprised a three-electrode configuration, consisting of a Pt/Rh gauze working electrode, a Pt wire secondary

(32) Fazlur-Rahman, A. K.; Verkade, J. G. *Inorg. Chem.* **1992**, *31*, 2064.

(33) IUPAC-Guidlines *Pure Appl. Chem.* **2001**, *73*, 1795.
(34) Cosier, J.; Glazer, A. M. *J. Appl. Crystallogr.* **1986**, *19*, 105.
(35) Area Detector Absorption Correction SADABS. In *Version 6.01 ed.*; Bruker AXS Inc.: Madison, WI, 1996.
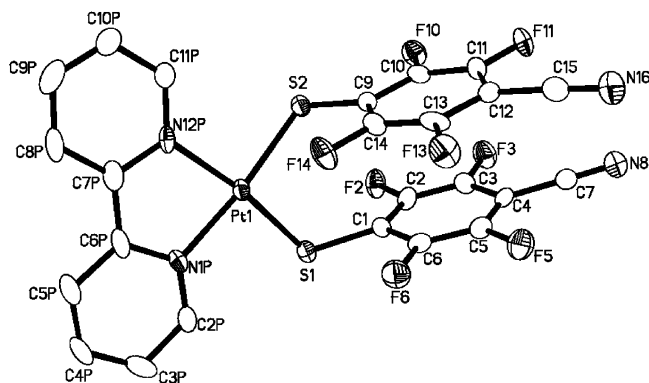(36) Sheldrick, G. M. *SHELXS-97, Acta Crystallogr., Sect. A* **1990**, *46*, 467.
(37) Sheldrick, G. M. *SHELXL-97*; University of Göttingen: Göttingen, Germany, 1997.
(38) Gagné, R. R.; Koval, C. A.; Lisensky, G. C. *Inorg. Chem.* **1980**, *19*, 2854.
(39) (a) Krejčik, M.; Danek, M.; Hartl, F. *J. Electroanal. Chem., Interfacial Electrochem.* **1991**, *313*, 243. (b) Murray, R. M.; Heineman, W. R.; O'Dom, G. W. *Anal. Chem.* **1967**, *39*, 1666.

Figure 1. The molecular structure of Pt(bpy)(4-CN−C$_6$F$_4$S)$_2$ showing the atom numbering scheme. Anisotropic displacement parameters are shown at 50% probability level and hydrogen atoms are omitted for clarity. Selected bond lengths and angles (Å, deg): Pt1−N1P, 2.049(4); Pt1−N12P, 2.054-(4); Pt1−S1, 2.2823(13); Pt1−S2, 2.2963(13); N1P−Pt1−N12P, 79.77-(16); N1P−Pt1−S1, 92.58(12); N12P−Pt1−S1, 170.82(11); N1P−Pt1−S2, 173.56(12); N12P−Pt1−S2, 95.15(12); S1−Pt1−S2, 92.10(5).

Table 1. Crystal Data for Pt(bpy)(4-CN−C$_6$F$_4$S)$_2$, **2**

formula	C$_{24}$H$_8$F$_8$N$_4$PtS$_2$	V (Å^3)	1148.1(5)
molecular weight	763.55	Z	2
crystal system	triclinic	μ (Mo Kα) (mm^{-1})	6.382
space group	$P\bar{1}$	reflns collected	7283
T (K)	150(2)	unique reflns	5135
a (Å)	8.768(2)	data with $I > 2\sigma(I)$	4074
b (Å)	11.084(3)	R(int)	0.029
c (Å)	13.007(3)	R_1 (F) for $I > 2\sigma(I)$	0.0333
α (deg)	111.553(3)	wR$_2$ (F^2) for all data	0.0474
β (deg)	95.589(3),	$\Delta\rho_{max}$ (e/Å^3)	1.08
γ (deg)	98.220(3)	$\Delta\rho_{min}$ (e/Å^3)	−1.63

electrode (in a fritted PTFE sleeve), and a SCE, chemically isolated from the test solution via a bridge tube containing electrolyte solution and terminated in a porous frit. The potential at the working electrode was controlled by a Sycopel Scientific Ltd. DD10M potentiostat. The (spectro)electrochemical UV−vis data were recorded on a Perkin-Elmer Lambda 16 spectrophotometer. The cavity was purged with dinitrogen, and temperature control at the sample was achieved by flowing cooled dinitrogen across the surface of the cell. Sample solutions were prepared under an atmosphere of argon using Schlenk line techniques and contained 10^{-3} M test compound and 0.2 M [NBu$_4$][BF$_4$] as supporting electrolyte. The test species in solution was electrolyzed at constant potential, typically 100 mV more negative than $E_{p,c}$ for a reduction. The redox process was considered complete when consecutive spectra were identical.

The picosecond TRIR studies were performed on the PIRATE setup in the Rutherford Appleton Laboratory, details of which are described elsewhere.[40] Briefly, part of the output from a 1 kHz, 800 nm, 150 fs, 2 mJ Ti/Sapphire oscillator/regenerative amplifier was used to pump a white light continuum seeded BBO optical parametric amplifier (OPA). The signal and idler produced by this OPA were difference frequency mixed in a type I AgGaS$_2$ crystal to generate tunable mid-IR pulses (ca. 150 cm^{-1} full width at half maximum, 1 μJ). Second harmonic generation of the residual 800-nm light provided 400-nm pulses, which were used to excite the sample. Changes in IR absorption were recorded by normalizing the outputs from a pair of 64-element HgCdTe linear-IR array detectors on a shot-by-shot basis. 300 lines/mm gratings were used in the spectrographs to achieve a high spectral resolution (approximately 4 cm^{-1} in the 2200 cm^{-1} region).

Results and Discussion

Crystal Structure. The crystal structure of Pt(bpy)(4-CN−C$_6$F$_4$S)$_2$ is illustrated in Figure 1. It shows that the Pt coordination geometry is approximately square planar, with one 2,2′-bipyridyl and two 4-cyano-perfluorothiophenolate ligands coordinated to the Pt center. The two phenyl rings of the 4-cyano-perfluorothiophenolates are almost coplanar.

The angle between the planes of these two rings is 1.49(9)°, and they lie approximately normal to the plane of the bipyridyl rings [dihedral angles 82.26(5) and 81.72(5)°]. It is noteworthy that the fluorinated thiolate rings are π stacked in the solid state, as the X-ray structure of neither the related Pt^{II} disulfide complex with perfluorinated thiophenols, Pt-(CH$_3$SCH(CH$_3$)CH(CH$_3$)SCH$_3$)(C$_6$F$_5$S)$_2$,[28b] nor of the related Pt^{II} diimine complexes with non-perfluorinated thiolates show such interaction.[5b,16b]

The closest intermolecular Pt···Pt distance is 4.62 Å, the corresponding interplanar distance between the bipyridine moieties is 3.492(4) Å, and the offset is 2.089 Å. The two aromatic rings are offset by 1.02 Å and twisted by 28.6° in such a way as to favor π−π interactions. They are almost coplanar, the dihedral angle being only 2.9°. The centroid−centroid distance is 3.34 Å, and the perpendicular separation of the rings is 3.18 Å. The crystal data are listed in Table 1.

Electronic Absorption Spectra. The electronic absorption spectra of the Pt(NN)(4-X−C$_6$F$_4$−S)$_2$ compounds in room-temperature solutions exhibit a broad asymmetric absorption band of medium intensity in the visible region (Table 2, Figure 2). The energy of this lowest absorption is sensitive to the nature of the ligands and to the polarity of the solvent. In all of these complexes, the lowest absorption band shows a negative solvatochromic behavior (Figure 3a), i.e., a decrease in energy with a decrease of solvent polarity. There is a linear correlation between this energy and the solvent polarity parameter value based on the energy of either the metal−ligand charge transfer (MLCT) transition of W(CO)$_4$-(bpy)[41] or the {charge-transfer-to-diimine} transition in Pt-(dbbpy)(tdt) (dbbpy = 4,4′-di-*tert*-butyl-2,2′-bipyridine, tdt = toluene-3,4-dithiolate)[18] (see Figure 3b). The slope of the linear correlation based on the latter scale gives the solvatochromic shift; the values obtained for Pt(phen)(C$_6$F$_5$S)$_2$ (0.56 eV), Pt(bpy)(C$_6$F$_5$S)$_2$ (0.44 eV), Pt(bpy)(4-CN−C$_6$F$_4$S)$_2$ (0.41 eV), and Pt(phen)(4-CN−C$_6$F$_4$S)$_2$ (0.38 eV) are typical values of those reported for charge-transfer transitions in other Pt^{II} diimine thiolates.[18]

The asymmetry of the lowest absorption manifold becomes more pronounced with decreasing solvent polarity, with the lowest-energy shoulder finally resolving as an independent band in CCl$_4$ (Figure 3a). Similar behavior has previously been observed for other Pt(diimine)thiolates.[6,14,15,17,42] The different solvatochromic behavior exhibited by the compo-

(40) Towrie, M.; Grills, D. C.; Dyer, J.; Weinstein, J. A.; Matousek, P.; Barton, R.; Bailey, P. D.; Subramaniam, N.; Kwok, W. M.; Ma, C.; Phillips, D.; Parker, A. W.; George, M. W. *Appl. Spectrosc.* **2002**, *57*, 367.

(41) Manuta, D. M.; Lees, A. J. *Inorg. Chem.* **1983**, *22*, 3825.
(42) Larionov, O.; Weinstein, J. A.; Zheligovskaya, N. N.; Mel'nikov, M. Y. *Russ. J. Coord. Chem., Engl. Transl.* **1999**, 45.

Table 2. The Position (λ_{max}), Extinction Coefficient (ϵ), and the Solvatochromic Shift ($\Delta\nu$) for the Lowest Absorption Band in Pt^{II}(diimine)(bis)thiolates **1**−**4** and Related Compounds at 298 K and Absorption Maxima for Their Electrochemically Generated Reduction Products (at 273 K in DMF unless stated otherwise)

| compound	λ_{max}/nm (ϵ/10^3 M^{-1} cm^{-1})	$\Delta\nu$/eV	UV−vis absorption maxima of the reduced products/nm
Pt(bpy)(C$_6$H$_5$S)$_2$[a]	498 (2.14[b])		271, 364, 454, 484, 706, 787
Pt(bpy)(C$_6$F$_5$S)$_2$, **1**	457 (3.20)	0.44	281, 314, 339, 384, 412, 533, 577, 622 very broad, 753
Pt(bpy)(4-CN−C$_6$F$_4$S)$_2$, **2**	444 (2.96)	0.37	367, 411, 460, 495, from 570 development to the NIR region
Pt(phen)(C$_6$F$_5$S)$_2$, **3**	471 (3.18)	0.56	280, 312, 383, 410, 534, 577, 631 tailing to 800
Pt(phen)(4-CN−C$_6$F$_4$S)$_2$, **4**	452 (2.20)	0.38	366, 410, 526, 571, broad manifold centered at 632 tailing to 800
Pt(phen)Cl$_2$	390 (3.56)		310, 335, 377, 437, 530, 572, 634 (very broad), 759

[a] From ref 14. [b] At 512 nm in CH$_2$Cl$_2$.
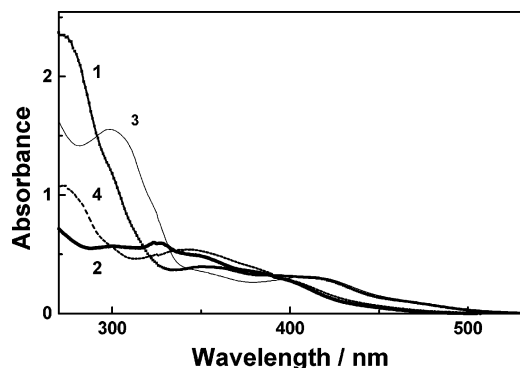
Figure 2. Electronic absorption spectra of **1**−**4** in DMF at room temperature.
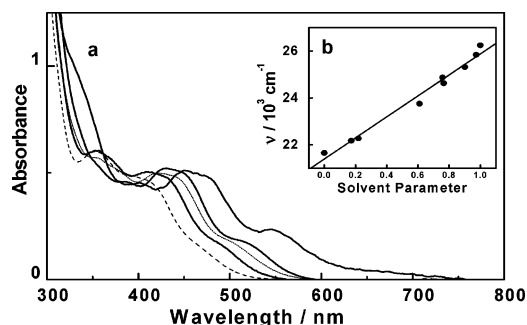
Figure 3. (a) Absorption spectra of Pt(phen)(C$_6$F$_5$S)$_2$, **3**, as a function of solvent polarity. In the order of decreasing energy of the lowest absorption band the solvents are DMSO (dashed line), C$_2$H$_4$Cl$_2$ (solid line), CHCl$_3$ (dotted line), C$_6$H$_6$ (solid line), and CCl$_4$ (solid line). (b) A plot of energy of the lowest absorption band of Pt(phen)(C$_6$F$_5$S)$_2$, **3**, as a function of solvent parameter[18] for DMSO, CH$_3$CN, DMF, C$_2$H$_4$Cl$_2$, CH$_2$Cl$_2$, CHCl$_3$, C$_6$H$_6$, C$_7$H$_8$, and CCl$_4$.

nents of the lowest energy absorption manifold observed suggests that more than one electronic transition is responsible for this band envelope.

Two possible assignments for the lowest absorption band in this absorption manifold can be envisaged, HOMO−LUMO transition or a singlet−triplet satellite to singlet−singlet HOMO−LUMO transition, which would be of considerable oscillator strength due to the presence of a heavy Pt^{II} center. We tentatively prefer to assign this to the latter by comparison with the previous work on Pt(diimine)-(dithiolates), where dithiolate = 1,2-ethane-dithiolate or *meso*-1,2-diphenyl-1,2-ethanedithiolate.[6]

The electronic absorption spectra suggest involvement of orbitals centered at both diimine and thiolate ligands in the lowest electronic transition. The value of the extinction coefficient (Table 2) for the lowest absorption band suggests involvement of Pt d orbitals in this electronic transition,
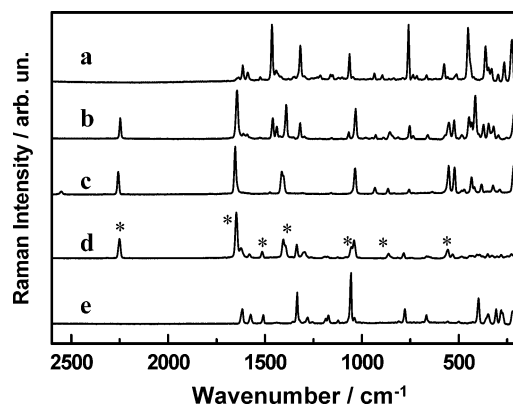
Figure 4. Raman spectra of polycrystalline samples obtained using 785 nm excitation: (a) Pt(phen)Cl$_2$; (b) Pt(phen)(4-CN−C$_6$F$_4$S)$_2$; (c) 4-CN−C$_6$F$_4$−SH; (d) Pt(bpy)(4-CN−C$_6$F$_4$S)$_2$; (e) Pt(bpy)Cl$_2$. The bands that are resonantly enhanced upon excitation of Pt(bpy)(4-CN−C$_6$F$_4$S)$_2$ at 457.9 and 488 nm (see text for details) are denoted with an asterisk.

which provides a better orbital overlap between the thiolate and the diimine moieties.

Resonance Raman Spectroscopy. To understand further the nature of the excited state, we have undertaken a resonance Raman investigation. The Raman spectra of the polycrystalline samples of compounds **2** and **4**, the precursor complexes Pt(bpy)Cl$_2$ and Pt(phen)Cl$_2$, and the free ligand 4-CN−C$_6$F$_4$SH collected under 785 nm excitation at room temperature are presented in Figure 4.

It is clear from Figure 4 that the Raman spectra of the mixed-ligand complexes are a superposition of the vibrations observed for the Pt(NN)Cl$_2$ complex and the thiolate ligand. An additional vibration was observed for the mixed-ligand complexes at 405 cm^{-1} (**2**) and 414 cm^{-1} (**4**), and we tentatively assign this band to ν(Pt−S), which was reported at 384 cm^{-1} for Pt(2-thpy)$_2$ (2-thpy = 2-thienyl-pyrdine).[43]

Most of the vibrations of Pt(bpy)Cl$_2$ that are resonantly enhanced under 457.9 nm excitation belong to the coordinated bpy.[44] In the 300−400 cm^{-1} region, Pt−Cl and Pt−N vibrations might also be anticipated.[45]

Pt(bpy)(4-CN−C$_6$F$_4$S)$_2$, 2. The resonance Raman spectra of Pt(bpy)(4-CN−C$_6$F$_4$S)$_2$ in KNO$_3$ pellets were obtained under 457.9 and 488 nm excitation. These spectra exhibit bands corresponding to the vibrational modes of the coordinated bpy-ligand, as has been shown previously by resonance Raman spectroscopy and normal coordinate

(43) Yersin, H.; Donges, D. *Top. Curr. Chem.* **2001**, *214*, 81.
(44) Hartl, F.; Snoeck, T. L.; Stufkens, D. J.; Lever, A. B. P. *Inorg. Chem.* **1995**, *34*, 3887 and references therein.
(45) Alkins, J. R.; Hendra, P. J. *J. Chem. Soc. A* **1967**, 1325.

Table 3. First $E_{1/2}^{0/-}$ and Second $E_{1/2}^{-/2-}$ Reduction Potentials and Anodic Half-Wave Potential $E_{p,a}$ Obtained for 1 mM Solutions of Pt^{II}(diimine)(bis)thiolates **1–4** in DMF at 298 K in the Presence of 0.2 M [Bu$_4$N][BF$_4$] (under 100 mV/s scan rate unless stated otherwise)

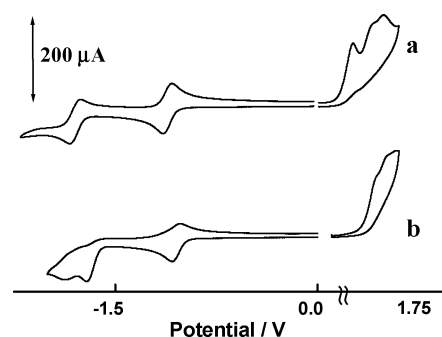|	thiolate	diimine	$E_{1/2}^{0/-}$ (ΔE)[a]/V	ΔE for Fc/Fc$^+$/mV	$E_{1/2}^{-/2-}$/V	$E_{p,a}$/V
1	C$_6$F$_5$S$-$	Bpy	-1.60 r (70)	70	-2.29 (82)	$+0.77$, $+0.99$ sh
2	4-CN$-$C$_6$F$_4$S$-$	Bpy	-1.54 r (70)	70	-2.14 (136) qr[c]	$+0.95$ sh, $+1.02$ sh
2[e]	4-CN$-$C$_6$F$_4$S$-$[e]	Bpy	-1.57 r (80)	90		
	C$_6$H$_5$S$-$[b]	Bpy	-1.72		-2.37	$+0.22$
	4-Me$_2$N$-$C$_6$H$_4$S$-$[b]	Bpy	-1.78		-2.41	-0.23
	Pt(bpy)Cl$_2$[b]		-1.64		-2.30[f]	$+0.67$
3	C$_6$F$_5$S$-$	phen	-1.61 qr (80)	70	-2.35 (90)[c]	$+0.78$ and $+0.99$
4	4-CN$-$C$_6$F$_4$S$-$	phen	-1.54 qr (70)	70	-2.32[d]	$+0.99$ and $+1.07$
	Pt(phen)Cl$_2$		-1.61 (80)	70		$+0.82$

[a] Potentials are measured vs SCE, quoted vs Fc/Fc$^+$; anodic/cathodic peak separation in mV is given in parentheses. [b] From ref 14. [c] Has a wave at reversed scan at scan rates >100 mV. [d] Multireduction process. [e] In CH$_2$Cl$_2$, 0.4 M [Bu$_4$N][BF$_4$]. [f] Chemically irreversible.

analysis.[14,44,46] There are also bands at 1631, 1394, 1379, and 1040 cm^{-1} in the resonance Raman spectrum of Pt(bpy)-(4-CN$-$C$_6$F$_4$S)$_2$, which were not seen for either Pt(bpy)Cl$_2$ or Pt(bpy)(PhS)$_2$.[14] All of these vibrations are seen in the Raman spectrum of the corresponding perfluorothiolate ligand (Figure 4). The 1394 and/or 1379 cm^{-1} bands are tentatively assigned to a mode with a large contribution from the C$-$F stretch. (The C$-$F vibration frequency was reported as 562 and 1491 cm^{-1} for C$_6$F$_6$,[47] 586 and 1410 cm^{-1} for C$_6$Cl$_3$F$_3$,[47] 580 and 1354 cm^{-1} for C$_6$H$_3$F$_3$,[47] and 1323 cm^{-1} for 3-F$-$(CF$_3$)-C$_6$H$_4$.)[48] The 1040-cm^{-1} band, which is also observed in the resonance Raman spectrum of [Pt(mnt)$_2$]$^{2-}$ (mnt = 1,2-maleonitrile$-$dithiolate),[49] is likely to be due to a mode with a significant amount of the C=C stretch of perfluorinated thiophenol.

A strong enhancement of the 2239-cm^{-1} band, which is assigned to the vibration of the CN group of the thiolate ligand, is noteworthy since this indicates the involvement of the thiolate ligand modes in the electronic transition studied.

The resonance Raman spectrum of Pt(bpy)(4-CN$-$C$_6$F$_4$S)$_2$ also displays a number of weak bands, which are not present in the Pt(bpy)Cl$_2$ spectrum. We assigned these to the thiophenol ring vibrations (892 and 1005 cm^{-1}), to C$-$F vibrations (531 and 556 cm^{-1}), and to the C$-$S vibration (871 cm^{-1}). The 892- and 1005-cm^{-1} bands were detected in the resonance Raman spectrum of [Pt(bpy)(PhS)$_2$][14] and are present as medium intensity bands in Raman spectra of C$_6$F$_5$SH[49] and 4-CN$-$C$_6$F$_4$SH. C$_6$F$_5$SH displays intense Raman bands at 583 and 510 cm^{-1};[50] liquid C$_6$F$_6$ at 542, 562, and 745 cm^{-1};[51] and 4-CN$-$C$_6$F$_4$SH at 521 and 552 cm^{-1}. The ν(CS) assignment has been made for the 866-cm^{-1} band of medium intensity observed in the Raman spectra of C$_6$F$_5$SH[50] and was also observed for 4-CN$-$C$_6$F$_4-$SH and for the 880 cm^{-1} band of [Ni(baba)(mnt)] and [Pd-

(46) (a) Forster, M.; Hester, R. E. *Chem. Phys. Lett.* **1981**, *81*, 42. (b) Mallick, P. K.; Danzer, G. D.; Strommen, D. P.; Kincaid, J. R. *J. Phys. Chem.* **1988**, *92*, 5620.
(47) Yumura, T.; Koga, M.; Hoshikawa, H.; Nibu, Y.; Shimada, R.; Shimada, H. *Bull. Chem. Soc. Jpn.* **1998**, *71*, 349.
(48) Yadav, R. A.; Singh, I. S. *Indian J. Pure Appl. Phys.* **1982**, *20*, 677.
(49) Clark, R. J. H.; Tortule, P. C. *J. Chem. Soc., Dalton Trans.* **1977**, 2142.
(50) Green, J. H. S.; Harrison, D. J.; Stockley, C. P. *Spectrochim. Acta, Part A* **1977**, *33A*, 423.
(51) Abramowitz, S.; Levin, I. W. *Spectrochim. Acta, Part A* **1970**, *26A*, 2261.
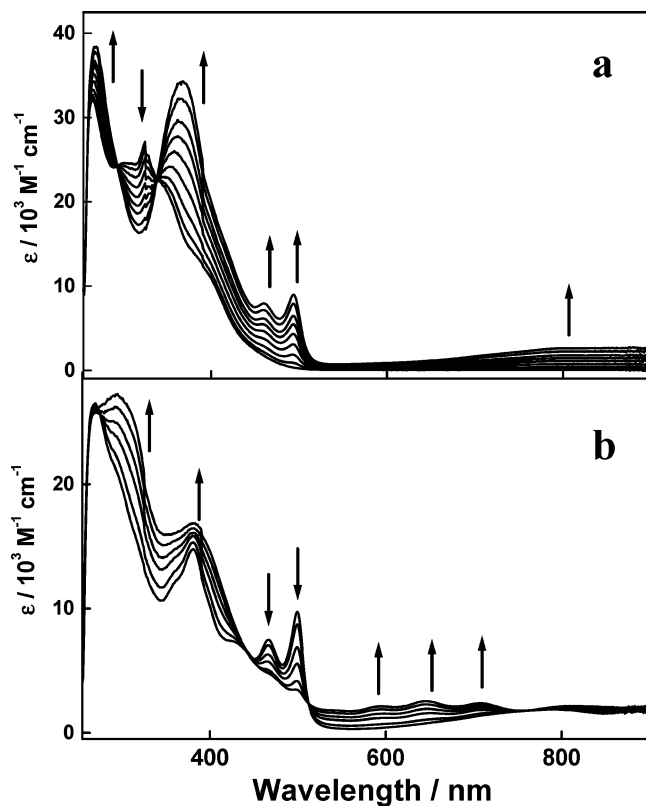
Figure 5. Cyclic voltammograms of Pt(bpy)(C$_6$F$_5$S)$_2$ (a) and Pt(bpy)(4-CN$-$C$_6$F$_4$S)$_2$ (b) obtained in 1 mM solutions in DMF, containing 0.2 M of [^{n}Bu$_4$N][BF$_4$], at 298 K (scan rate 100 mV/s).

(baba)(mnt)] (baba = biacetylbisaniline). Thus, resonance Raman data show the involvement of both diimine and thiolate ligand vibrational modes in the lowest electronic transition. The involvement of the thiolate ligand is clearly seen by the strong ν(CN) resonance at 2234 cm^{-1}, the intensity of which increases on changing from 457.9 to 488 nm excitation, corresponding to an increase in absorbance along the lowest absorption band. This demonstrates a difference between the localization of electronic density in the excited state of Pt^{II} diimines with perfluorinated thiolates compared to Pt(diimine)(bis)thiolates, since the latter do not show any considerable enhancement of thiolate vibrations upon excitation along the lowest absorption band.

(Spectro)electrochemistry. To probe the nature of the frontier orbitals and elucidate the electrochemical properties of **1–4**, cyclic voltammetry and UV$-$vis spectroelectrochemical studies have been performed. The redox potentials are listed in Table 3.

Reduction. The cyclic voltammograms of compounds **1** and **2** in DMF are shown in Figure 5. The first reduction is a one-electron process, electrochemically reversible for the bpy complexes **1** and **2** and quasi-reversible for the phen complexes **3** and **4** under the experimental conditions applied. The value of the first reduction potential is largely unaffected by the nature of the thiolate or diimine and is close to the value of the first reduction potential for the corresponding Pt(diimine)Cl$_2$ (Table 3). This suggests that the LUMO is mainly localized on the diimine ligand. Substitution of $-$C$_6$F$_5$S$-$ with 4-CN$-$C$_6$F$_4-$S$-$ introduces a small (ca. 60 mV) positive shift in the first reduction potential of the phenanthroline and bipyridine complexes due to the introduction of the more-electron-withdrawing thiolate.

Figure 6. (a) UV−vis spectral changes accompanying the first reduction of a 1 mM solution of Pt(bpy)(4-CN−C$_6$F$_4$−S)$_2$ in DMF, containing 0.2 M of [^{n}Bu$_4$N][BF$_4$], 273 K. Applied potential −1.20 V vs SCE. (b) UV−vis spectral changes accompanying the second reduction of a 1 mM solution of Pt(bpy)(C$_6$F$_5$−S)$_2$ in DMF, containing 0.2 M of [^{n}Bu$_4$N][BF$_4$], 223 K. Applied potential −1.98 V vs S.C.E.

UV−vis (spectro)electrochemical investigations into the nature of the first reduction process have been performed in order to obtain further information about localization of the LUMO in **1**−**4**. The absorption maxima of the electrochemically generated radical anions of **1**−**4** and Pt(phen)Cl$_2$ in DMF at 273 K are listed in Table 2. As a typical example, the spectral changes which accompany the first reduction process of Pt(bpy)(4-CN−C$_6$F$_4$S)$_2$ are shown in Figure 6a. The UV−vis spectra of the [Pt(bpy)(4-CN−C$_6$F$_4$S)$_2$]$^{•−}$ and [Pt(bpy)(C$_6$F$_5$S)$_2$]$^{•−}$ radical anions possess spectral features characteristic[52] of an intraligand electronic transition in a coordinated bpy$^{•−}$ radical anion. Similarly, the UV−vis spectra of [Pt(phen)(4-CN−C$_6$F$_4$S)$_2$]$^{•−}$ and [Pt(phen)-(C$_6$F$_5$S)$_2$]$^{•−}$ show spectral profiles comparable to that of [Pt(phen)Cl$_2$]$^{•−}$ (Table 2). Thus, (spectro)electrochemical data support the conclusion that the LUMO in **1**−**4** is mainly centered on the π_1* orbital of the corresponding diimine ligand.

The values of the second reduction potentials of **1**−**4** (Table 3) are very similar to each other. The second reduction process shows no return wave for either of the phen compounds, **3** and **4**, under scan rates of ≤300 mV/s. For Pt(bpy)(C$_6$F$_5$S)$_2$, the second reduction is a quasi-reversible

process. However, introduction of the strongly-electron-withdrawing CN-substituent to the thiolate ligand of Pt(bpy)-(4-CN−C$_6$F$_5$S)$_2$ leads to a less defined character of reduction of [Pt(bpy$^{•−}$)(4-CN−C$_6$F$_4$S)$_2$], with at least two overlapping processes.

A spectroelectrochemical investigation into the nature of the second reduction process of Pt(bpy)(4-CN−C$_6$F$_4$S)$_2$ and Pt(bpy)(C$_6$F$_5$S)$_2$ has been performed. At 273 K, the products of double reduction of **1** and **2** were unstable on the time scale of the experiment. This observation is consistent with the previously reported data on the instability of products of double reduction of Pt(4,4′-X$_2$-bpy)Cl$_2$ in the temperature range 273−243 K, unless the substituent X is strongly electron withdrawing.[53a] Cooling the solution of **1** to 223 K allowed the UV−vis spectrum of the doubly reduced [Pt(bpy)(C$_6$F$_5$S)$_2$]$^{2−}$ (Figure 6b) to be obtained (with ca. 95% regeneration of the initial spectrum after reoxidation). The spectrum of the doubly reduced **1** displays bands at 382, 592, 645, and 706 nm and gradually increasing absorption toward the NIR region, indicating that the second reduction in Pt-(bpy)(C$_6$F$_5$S)$_2$ is likely to be directed to the bpy-ligand. However, the second reduction of Pt(bpy)(4-CN−C$_6$F$_4$S)$_2$ remains chemically irreversible under the same conditions (227 K). This may be due to a close overlap between second and third reductions, one of which might be centered on the electron-withdrawing thiolate ligand.

Oxidation. The compounds studied show an irreversible oxidation (Figure 5) at scan rates of ≤300 mV/s at room temperature. Similar behavior has been reported for Pt(bpy)-(4-X−C$_6$H$_4$S)$_2$ complexes with X = H, MeO, or NO$_2$.[14] The diimine ligands have essentially no effect on the values of the oxidation potentials $E_{p,a}$. However, the $E_{p,a}$ values are strongly affected by the donor capability of the thiolate ligand; substitution of −C$_6$F$_5$S− with 4-CN−C$_6$F$_4$−S− shifts the oxidation potentials ca. 200 mV more positive (Table 3). The previously reported Pt(bpy)(C$_6$H$_5$S)$_2$ and Pt(bpy)-(Me$_2$N−C$_6$H$_4$−S)$_2$[14] complexes contain more electron-donating thiolate ligands than those used in the present study and hence display less positive $E_{p,a}$ values for the first irreversible oxidation process (Table 3). This indicates that the HOMO in **1**−**4** is mostly centered on the thiolate ligand.

Time-Resolved Infrared Spectroscopy. The ground-state IR spectrum of **2** in CH$_2$Cl$_2$ at room temperature exhibits a single ν(CN) band at 2240 cm^{-1} (Figure 7a). 400-nm (150-fs) excitation leads to an instantaneous bleaching of this parent absorption together with the formation of a new band at ca. 2232 cm^{-1}. Picosecond TRIR spectra recorded at several pump−probe delays between 1 and 500 ps are shown in Figure 7b.

The small negative shift of the CN vibration observed in the TRIR spectra (ca. 8 cm^{-1}) (Figure 7b) is consistent with a depopulation of the bonding π-orbital of the CN group upon promotion to the excited state. This therefore supports

(52) (a) Krejčik, M.; Vlček, A. A. *J. Electroanal. Chem., Interfacial Electrochem.* **1991**, *313*, 243. (b) Vichova, J.; Hartl, F.; Vlček, A. *J. Am. Chem. Soc.* **1992**, *114*, 10903. (c) Noble, B. C.; Peacock, R. D. *Spectrochim. Acta, Part A* **1990**, *46*, 407.

(53) (a) McInnes, E. J. L.; Farley, R. D.; Rowlands, C. C.; Welch, A. J.; Rovatti, L.; Yellowlees, L. J. *J. Chem. Soc., Dalton Trans.* **1999**, 4203. (b) Kaim, W.; Dogan, A.; Wanner, M.; Klein, A.; Tiritiris, I.; Schleid, T.; Stufkens, D. J.; Snoeck, T. L.; McInnes, E. J. L.; Fiedler, J.; Zalis, S. *Inorg. Chem.* **2002**, *41*, 4139.
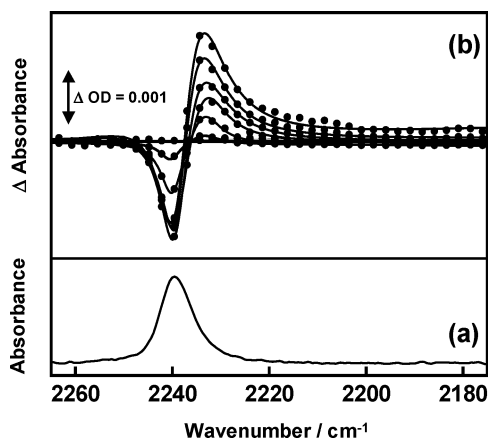
Figure 7. (a) Ground-state infrared spectrum of a 1 mM CH_2Cl_2 solution of Pt(bpy)(4-CN−C$_6$F$_4$−S)$_2$ (**2**) at 298 K. (b) Time-resolved infrared spectra obtained from this solution at 1-, 2-, 5-, 15-, 30-, 60-, and 500-ps time delays after 150-fs 400-nm pulse excitation. Solid lines represent Lorentzian fits to the data.
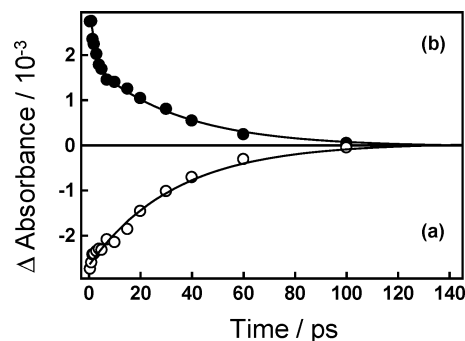
the assignment of the HOMO as being mostly thiolate centered and the lowest electronic transition in Pt(bpy)(4-CN−C$_6$F$_4$−S)$_2$ being from the thiolate moiety to the α-diimine.

The changes in the energy of the cyanide stretching frequencies upon promotion to the excited state for various transition-metal complexes containing a CN group directly bound to the metal center have been discussed elsewhere.[23,54]

An alternative interpretation could have been to attribute this small negative shift of ν(CN) to a population of the CN π* antibonding orbital. This is unlikely since it requires a thiolate-centered LUMO. As discussed above, the absorption spectrum of the electrochemically reduced species corresponds to a coordinated bpy radical anion, indicating that the LUMO is centered on the bpy ligand in Pt(bpy)(4-CN−C$_6$F$_4$−S)$_2$. This is also supported by the electrochemical data on reduction potentials and absorption spectra.

The spectra were fitted, assuming a Lorentzian band shape (solid lines in Figure 7b), allowing the determination of the areas of the bleach and transient at each time delay. A small narrowing of the transient band, observed at early time delays (Figure 7b), is assigned to early relaxation processes, associated with the decay of "hot" vibrational modes initially formed upon excitation. The production of "hot" excited states and their effect on the IR spectrum is well established and has been discussed in detail.[55]

The very small negative shift observed for the ν(CN) stretch is consistent with organic peripheral IR reporters generally exhibiting smaller shifts in the excited state than metal carbonyls or cyanides, possibly due to a larger degree of delocalization of electronic density. Typically, metal

(54) (a) Bignozzi, C. A.; Argazzi, R.; Schoonover, J. R.; Gordon, K. C.; Dyer, B. R.; Scandola, F. *Inorg. Chem.* **1992**, *31*, 5260. (b) Roncaroli, F.; Baraldo, L. M.; Slep, L. D.; Olabe, J. A. *Inorg. Chem.* **2002**, *41*, 1930. (c) Turner, J. J. *Coord. Chem. Rev.* **2002**, *230*, 213. (d) Macatangay, A. V.; Mazzetto, S. E.; Endicott, J. F. *Inorg. Chem.* **1999**, *38*, 5091. (e) Schoonover, J. R.; Bignozzi, C. A.; Meyer, T. J. *Coord. Chem. Rev.* **1997**, *165*, 239.
(55) (a) Dougherty, T. P.; Heilweil, E. J. *Chem. Phys. Lett.* **1994**, *227*, 19. (b) Hamm, P.; Ohline, S. M.; Zinth, W. *J. Chem. Phys.* **1997**, *106*, 519. (c) Marks, S.; Cornelius, P. A.; Harris, C. B. *J. Chem. Phys.* **1980**, *73*, 3069.

Figure 8. Kinetic traces obtained from the peak heights of the parent band at 2240 cm^{-1} (a) and transient decay at 2232 cm^{-1} (b) in picosecond TRIR experiment: ●, experimental data; solid lines, monoexponential and biexponential fits to the data, respectively.

carbonyls exhibit a 50−60 cm^{-1} positive shift of the ν(CO) stretch[21] upon promotion to the MLCT state. In contrast, organic carbonyl reporters in Ru^{II},[25] Re^I,[3] or Pt^{II} [26] complexes bearing 2,2′-bpy-4,4′-(C(O)OR)$_2$ ligands show only a −25 to −30 cm^{-1} shift upon promotion to the MLCT excited state.

The TRIR kinetic traces for parent recovery (Figure 8a) and transient decay (Figure 8b) have been plotted as a height of the corresponding band versus pump−probe delays. Within 200 ps, the bleach and transients have completely recovered back to the baseline. The parent absorption recovers monoexponentially, with a rate constant 3.0 (±0.3) × 10^{10} s^{-1}, as is represented in Figure 8a. However, the transient absorption decays in a biexponential fashion (Figure 8b), with the rate constants of 4.7 (±1.0) × 10^{11} and 2.9 (±0.4) × 10^{10} s^{-1}. The slower component agrees well with the rate constant for the bleach recovery. We therefore tentatively attribute these two decay constants to vibrational cooling 2.1 (±0.5 ps) and back-electron-transfer processes in the {charge-transfer-to-diimine} excited state of Pt(bpy)-(4-CN−C$_6$F$_4$−S)$_2$.

The lifetime of vibrational cooling has been reported[56] to be ca. 5 ps for [Ru^{III}(4,4′-dimethyl-2,2′-bpy$^{•-}$)$_3$]$^{2+*}$ and ca. 2 ps for [Ru^{III}(4,4′-diphenyl-2,2′-bpy$^{•-}$)$_3$]$^{2+*}$ in CD$_3$CN. Recently, we have reported the lifetime of vibrational cooling of Pt(4,4′-(C(O)OEt)$_2$-2,2′-bpy)Cl$_2$ as 2.3 (±0.3) ps in the MLCT excited state in CH$_2$Cl$_2$ solution at room temperature.[26] The 2-ps lifetime obtained in the present study is in reasonable agreement with the values for the Ru^{II} and Pt^{II} complexes mentioned above.

The Nature of the Lowest Excited State in the Pt-(diimine)(bis)perfluorothiolate Complexes 1−4. There are four main orbital manifolds to consider in respect to localization of HOMO and LUMO in the complexes under study: π-system of the diimine ligand, Pt atom d-orbitals, S atom lone pairs, and the π-system of the perfluorinated thiolate rings.

The lowest UV−vis absorption band of the studied compounds displays negative solvatochromic behavior, characteristic of the charge-transfer nature of the correspond-

(56) (a) Damrauer, N. H.; McCusker, J. K. *J. Phys. Chem. A* **1999**, *103*, 8440. (b) Yeh, A. T.; Shank, C. V.; McCusker, J. K. *Science* **2000**, *289*, 935. (c) Monat, J. E.; McCusker, J. K. *J. Am. Chem. Soc.* **2000**, *122*, 4092.

ing transition. The influence of both ligands on the absorption energy suggests participation of both ligands in this electronic transition. This is supported by resonance Raman enhancement of both diimine and thiolate intraligand vibrations upon excitation along the lowest absorption band.

Absorption spectra of the electrochemically generated monoreduced species correspond to the coordinated diimine radical anions, indicating that the LUMO is predominantly centered on the diimine ligand in Pt(diimine)(4-X$-$C$_6$F$_4-$S)$_2$ **1**$-$**4**. The first reduction potentials of **1**$-$**4** are only slightly affected by the changes in the thiolate ligands and are close to the value of the reduction potential of the corresponding Pt(diimine)Cl$_2$. This supports the assignment of the LUMO as mostly localized on the diimine ligand. A considerable contribution of Pt d orbitals in the LUMO has been proposed for the Pt(4,4$'$-X$_2$-2,2$'$-bpy)Cl$_2$ complexes on the basis of an extensive EPR study.[53a] A similar contribution has been reported for the singly-occupied MO of the electrochemically generated radical anion of Pt(2,2$'$-bipyrimidine)Cl$_2$.[53b] A small negative shift of the CN vibration compared to the ground state, observed in the TRIR spectrum of Pt(bpy)(4-CN$-$C$_6$F$_4$S)$_2$, is consistent with the bpy-centered assignment of the LUMO since it reflects a depopulation of the bonding π-orbital of the CN group upon promotion to the excited state.

The energy of the lowest absorption in Pt(diimine)(bis)thiolate and the value of the oxidation potential, $E_{p,a}$, both decrease with an increase of the thiolate ligand donor ability in the order 4-CN$-$C$_6$F$_4$$-$S $<$ C$_6$F$_5$S$-$ $<$ C$_6$H$_5$S$-$ $<$ 4-Me$_2$N$-$C$_6$H$_4$S$-$. This indicates that the HOMO is mainly thiolate in character. The same conclusion has been drawn previously for, e.g., Pt(bpy)L, where L = toluene dithiolate or catecholate.[57] An alternative term, {charge-transfer-to-diimine}, was introduced by Eisenberg[8,17,18,58] while discussing the nature of the lowest excited state in a large library of Pt(diimine)(dithiolates). This definition assumes a substantial contribution of Pt d orbitals in the HOMO and was later accepted for some Pt(diimine)(bis)thiolates. For the complexes in this study, the Pt d orbitals contribution in the HOMO is supported by the significant value of the extinction coefficient for the lowest electronic transition.

Thus, we assign the lowest electronic transition in Pt-(diimine)(4-X$-$C$_6$F$_4-$S)$_2$ to a charge-transfer transition from the mixed platinum/thiolate moiety to the α-diimine. The dynamics of this {charge-transfer-to-diimine} lowest excited state are governed by vibrational cooling (ca. 2 ps) and back-electron-transfer (35 ps) processes.

Conclusions

A combined (spectro)electrochemical, resonance Raman, and TRIR study of a series of Pt^{II} diimine complexes with perfluorinated thiolate ligands has suggested that the HOMO is mainly composed of thiolate(π)/S(p)/Pt(d) orbitals and the LUMO is predominantly localized on the π* (diimine) orbital. The introduction of fluorine substituents on the thiolate moiety possibly leads to a more pronounced contribution of the intrathiolate modes to the HOMO as manifested by the enhancement of the thiolate ring vibrations, C$-$F vibrations, and the vibration of the CN-substituent on the thiolate moiety in the resonance Raman spectra. This contrasts with the observation for the nonfluorinated thiolate analogue where no such enhancement was seen.[14] The dynamics of the lowest {charge-transfer-to-diimine} excited state on the picosecond time scale are governed by ca. 2-ps vibrational cooling and 35-ps back electron transfer.

Supporting Information Available: The table listing Raman data for Pt(diimine)(bis)thiolates **2** and **4** and related compounds, obtained under 785 nm excitation, and a CIF file for **2** are also available. This material is available free of charge via the Internet at http://pubs.acs.org.

IC026286L

(57) Kumar, L.; Puthraya, K. H.; Srivastava, T. S. *Inorg. Chim. Acta* **1984**, *86*, 173.
(58) Cummings, S. D.; Eisenberg, R. *Inorg. Chim. Acta* **1996**, *242*, 225.